

Stasevich, T. J.;
Einstein, T. L.;
Zia, R. K. P.;
Giesen, M.; Ibach,
H.; Szalma, F.,
"Effects of next-
nearest-neighbor
interactions on
the orientation
dependence of step
stiffness:

Reconciling theory
with experiment
for Cu(001),"

Phys. Rev. B **70**,
245404 DOI:

http://
dx.doi.org/10.1103

/
PhysRevB.70.245404

Effects of next-nearest-neighbor interactions on the orientation dependence of step stiffness: Reconciling theory with experiment for Cu(001)

T. J. Stasevich* and T. L. Einstein†

Department of Physics, University of Maryland, College Park, Maryland 20742-4111, USA

R. K. P. Zia

Department of Physics, Virginia Polytechnic Institute and State University, Blacksburg, Virginia 24601, USA

M. Giesen and H. Ibach

Institut für Schichten und Grenzflächen, ISG, Forschungszentrum Jülich, D 52425 Jülich, Germany

F. Szalma

Department of Physics, University of Maryland, College Park, Maryland 20742-4111, USA

(Received 4 August 2004; published 3 December 2004)

Within the solid-on-solid (SOS) approximation, we carry out a calculation of the orientational dependence of the step stiffness on a square lattice with nearest- and next-nearest-neighbor interactions. At low temperature our result reduces to a simple, transparent expression. The effect of the strongest trio (three-site, nonpairwise) interaction can easily be incorporated by modifying the interpretation of the two pairwise energies. The work is motivated by a calculation based on nearest neighbors that underestimates the stiffness by a factor of 4 in directions away from close-packed directions, and a subsequent estimate of the stiffness in the two high-symmetry directions alone that suggested that inclusion of next-nearest-neighbor attractions could fully explain the discrepancy. As in these earlier papers, the discussion focuses on Cu(001).

DOI: 10.1103/PhysRevB.70.245404

PACS number(s): 68.35.Md, 81.10.Aj, 05.70.Np, 65.80.+n

I. INTRODUCTION

At the nanoscale, steps play a crucial role in the dynamics of surfaces. Understanding step behavior is therefore essential before nanostructures can be self-assembled and controlled. In turn, step stiffness plays a central role in our understanding of how steps respond to fluctuations and driving forces. It is one of the three parameters of the step-continuum model,¹ which has proved a powerful way to describe step behavior on a coarse-grained level, without recourse to a myriad of microscopic energies and rates. As the inertial term, stiffness determines how a step responds to interactions with other steps, to atomistic mass-transport processes, and to external driving forces. Accordingly, a thorough understanding of stiffness and its consequences is crucial.

The step stiffness $\tilde{\beta}$ weights deviations from straightness in the step Hamiltonian. Thus, it varies inversely with the step diffusivity, which measures the degree of wandering of a step perpendicular to its mean direction. This diffusivity can be readily written down in terms of the energies ϵ_k of kinks along steps with a mean orientation along close-packed directions [$\langle 110 \rangle$ for an fcc (001) surface]: in this case, all kinks are thermally excited. Conversely, experimental measurements of the low-temperature diffusivity (via the scale factor of the spatial correlation function) can be used to deduce the kink energy. A more subtle question is how this stiffness depends on the azimuthal misorientation angle, conventionally called θ and measured from the close-packed direction. In contrast to $\theta=0$ steps, even for temperatures much below ϵ_k , there are always a non-vanishing number of kinks,

the density of which are fixed by geometry (and so are proportional to $\tan \theta$). In a bond-counting model, the energetic portion of the step free energy per length [or, equivalently, the line tension, since the surface is maintained at constant (zero) charge²] $\beta(\theta)$ is canceled by its second derivative with respect to θ , so that the stiffness is due to the entropy contribution alone. Away from close-packed directions, this entropy can be determined by simple combinatoric factors at low temperature T .³⁻⁵

Interest in this whole issue has been piqued by the recent finding by Dieluweit *et al.*⁶ that the stiffness as predicted in the above fashion, assuming that only nearest-neighbor (NN) interactions ϵ_1 are important, underestimates the values for Cu(001) derived from two independent types of experiments: direct measurement of the diffusivity on vicinal Cu surfaces with various tilts and examination of the shape of (single-layer) islands. The agreement of the two types of measurements assures that the underestimate is not an anomaly due to step-step interactions. In that work, the effect of next-nearest-neighbor (NNN) interactions ϵ_2 was crudely estimated by examining a general formula obtained by Akutsu and Akutsu,⁷ showing a correction of order $\exp(-\epsilon_2/k_B T)$, which was glibly deemed to be insignificant. In subsequent work the Twente group⁹ considered steps in just the two principal directions and showed that if one included an attractive NNN interaction, one could evaluate the step free energies and obtain a ratio consistent with the experimental results in Ref. 6. This group later extended their calculations¹⁰ to examine the stiffness.

To make contact with experiment, one typically first gauges the diffusivity along a close-packed direction and

from it extracts the ratio of the elementary kink energy ε_k to T . Arguably the least ambiguous way to relate ε_k to bonds in a lattice gas model is to extract an atom from the edge and place it alongside the step well away from the new unit indentation, thereby creating four kinks.¹¹ The removal of the step atom costs energy $3\varepsilon_1 + 2\varepsilon_2$ while its replacement next to the step recoups $\varepsilon_1 + 2\varepsilon_2$. Thus, whether or not there are NNN interactions, we identify $\varepsilon_k = -\frac{1}{2}\varepsilon_1 = \frac{1}{2}|\varepsilon_1|$ (since the formation of Cu islands implies $\varepsilon_1 < 0$); thus, as necessary, $\varepsilon_k > 0$. Note that for clarity we reserve the character ε for lattice-gas energies,¹² which are deduced by fitting this model to energies which can be measured, such as ε_k .

The goal of this paper is to compute the step line tension β and the stiffness $\tilde{\beta}$ as functions of azimuthal misorientation θ , when NNN (in addition to NN) interactions contribute. Since it is difficult to generalize the low-temperature expansion of the Ising model,^{3,4} we instead study the solid-on-solid (SOS) model, which behaves very similarly at low temperatures and at azimuthal misorientations that are not too large, but can be analyzed exactly even with NNN interactions. This derivation is described in Sec. II, with most of the calculational details placed in the Appendix. In Sec. III we derive a simple expression for the stiffness in the low-temperature limit, presented in Eq. (14). We also make contact with parameters relevant to Cu(001), for which this limit is appropriate. In Sec. IV we extend the formalism to encompass the presumably strongest trio (three-atom, non-pairwise) interaction, showing that its effect can be taken into account by shifting the pair energies in the preceding work. The final section offers discussion and conclusions.

II. NNN SOS MODEL ON A SQUARE LATTICE

Including NNN interactions in the low-temperature expansion of the square-lattice Ising model lifts the remarkable degeneracy of the model with just NN bonds. In that simple case, the energy of a path depends solely on the number of NN links, independent of the arrangement of kinks along it; thus, the energy of the ground state is proportional to the number of NN links of the shortest path between two points, and the entropy is related to the number of combinations of horizontal and vertical links that can connect the points.^{3,5} Including NNN interactions causes the step energy to become a function of both the length of the step and the number of its kinks, eliminating the simple path-counting result.⁵ It can then become energetically favorable for the step to lengthen rather than add another kink. This causes the NN energy levels to split in a nontrivial way, making it possible for a longer step to have a lower energy than a shorter step. A related complication is that the expansion itself depends on the relative strength of the NNN interaction: Instead of an expansion just in terms of $\exp(-|\varepsilon_1|/k_B T)$, the expansion also is in terms of $\exp(\varepsilon_2/2k_B T)$. Hence, to take the NNN expansion to the same order of magnitude as the NN expansion, an unspecified number of terms is required, depending on the size of the ratio $\varepsilon_2/\varepsilon_1$.

Since the NNN Ising model cannot be solved exactly and we cannot generalize the low- T expansion, we turn to an SOS model, which was used in earlier examinations of step

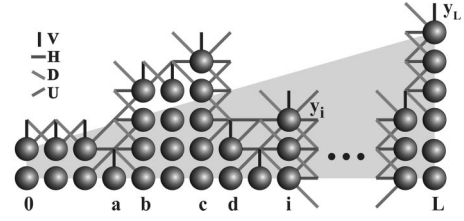


FIG. 1. A finite-sized step edge whose projected length is L . The step has height y_i at position i ($0 \leq i \leq L$). The height difference $y_L - y_0$ is fixed; thus, the step edge makes an angle θ with the horizontal axis, and has an overall slope m (shown as the top of the gray region). The energy of the step edge is found by counting the number of broken links required to form it. Here all NN and NNN broken links are shown.

problems, most notably in the seminal work of Burton, Cabrera, and Frank,¹³ and later used for steps of arbitrary orientation by Leamy, Gilmer, and Jackson.¹⁴ It was also applied to an interface of arbitrary orientation in a square-lattice Ising model.¹⁵

Although the SOS model can be treated exactly, the result is somewhat unwieldy. Fortunately, at low temperature—the appropriate regime for the experiments under consideration—the solution reduces to a simple expression.

A. Description of the model

Consider a step edge of projected length L separating an upper adatom-free region from a lower adatom-filled region (see Fig. 1). The step edge is completely described by specifying its height y_i at position i ($0 \leq i \leq L$). The energy of the step edge depends on the number of broken bonds required to form it. Let V and H represent the vertical and horizontal NN bond strengths divided by $k_B T$, and let U and D represent up-diagonal and down-diagonal NNN bond strengths over $k_B T$. Then the step-edge energy $E \equiv E(\{\Delta_i\})$ depends only on $\Delta_i \equiv y_i - y_{i-1}$.

For clarity, we consider two examples. First, if $\Delta_i = 3$ (as is the case between columns a and b in Fig. 1), then between positions i and $i+1$ there are 3 broken H links, 2 broken U links, and 4 broken D links. There are also 2 broken V links, but this number is independent of Δ_i , since every step-edge configuration of projected length L requires exactly L broken V links. Similarly, if $\Delta_i = -3$ (as is the case between columns c and d in Fig. 1), then there would be the same number of broken H links, but there would now be 4 broken U links and 2 broken D links (that is, the number of broken U and D links switch from the previous case). From these examples we see that, in general, there are $|\Delta_i|$ broken H links, $|\Delta_i - 1|$ broken U links, and $|\Delta_i + 1|$ broken D links. It therefore follows that the step-edge energy is

$$\frac{E(\{\Delta_i\})}{k_B T} = \sum_{i=1}^L (V + H|\Delta_i| + U|\Delta_i - 1| + D|\Delta_i + 1|) \equiv \sum_{i=1}^L K(\Delta_i). \quad (1)$$

Because we seek the orientation dependence of β and $\tilde{\beta}$, we constrain the step to have an overall offset $Y \equiv y_L - y_0$

$\equiv L \tan \theta = \sum_{i=1}^L \Delta_i$. (This constraint is represented in Fig. 1 by the shaded gray area. Equivalently, we specify that the overall slope of the step is $m \equiv \tan \theta$.) The constrained partition function is therefore

$$Z(Y) \equiv \sum_{\{\Delta\}} \delta\left(Y - \sum_{i=1}^L \Delta_i\right) e^{-E(\{\Delta_i\})/k_B T}, \quad (2)$$

where $\{\Delta\}$ is the set of all Δ_i each of which ranges over all integers. From $Z(Y)$ we can find the orientation dependence of the free energy $F(Y) = -k_B T \ln Z(Y)$, the *projected* free energy per length $f(m) = F(Y)/L$, and the line tension (or free energy per length) $\beta(\theta) = f(m) \cos \theta$ (since the step length is $L/\cos \theta$); hence, we can find the stiffness $\tilde{\beta}(\theta) = \beta(\theta) + \partial^2 \beta(\theta) / \partial \theta^2$.

For future reference, note that the process of extracting an atom from the step edge and replacing it alongside the edge, discussed in the penultimate paragraph of the Introduction, creates two pairs of $\Delta = +1$ and $\Delta = -1$, costing $4H$ according to Eq. (1) and removing a net of 2 NN bonds, so that $H = -\epsilon_1/2k_B T = \epsilon_k/k_B T$. Similarly, we compare the energies of two NN atoms, abutting (the lower side of) a step edge ($\{\Delta_i\} = 0$) at i_0 and either parallel or perpendicular to the edge. In the first case, $\Delta_{i_0} = +1$ and $\Delta_{i_0+2} = -1$, with an added energy of $2H + 2(U + D)$ according to Eq. (1). In the perpendicular case $\Delta_{i_0} = +2$ and $\Delta_{i_0+1} = -2$, implying an added energy of $4H + 4(U + D)$. Counting bonds we see that the parallel configuration has one more ϵ_1 bond and two more ϵ_2 bonds than the perpendicular configuration. Invoking $H = -\epsilon_1/2k_B T$, we see that $U + D = -\epsilon_2/k_B T$; if $U = D$, then $D = -\epsilon_2/2k_B T$. The factor-of-2 difference between broken links in Eq. (1) and broken bonds was noted (for H links) already in the classic exposition by Leamy *et al.*¹⁴ An alternate argument, presented over a decade ago,¹⁶ for this factor of 2 is that the ragged edge is created by severing bonds along the selected path through an infinite square. This leads to the formation of two complementary irregular boundary layers (with reverse values of $\{\Delta_i\}$, so that the associated energy of each is half that of the broken bonds).

B. Evaluation of the free energy

As detailed in the first part of the Appendix, the sum in the Fourier transform of $Z(Y)$, which we denote by $W(\mu)$, factorizes. Thus, it can be written as

$$W(\mu) = \exp[-Lg(i\mu)/k_B T],$$

where $g(i\mu)$ is the reduced Gibbs free energy per column. To evaluate the inverse transform, we exploit the saddle point method and obtain (see the Appendix for details)

$$Z(Y) \approx \exp\left[-L\left(\rho_0 \tan \theta + \frac{g(\rho_0)}{k_B T}\right)\right], \quad (3)$$

where the saddle point ($\mu_0 = -i\rho_0$) is defined implicitly by the stationarity condition

$$-\frac{g'(\rho_0)}{k_B T} = m \equiv \tan \theta. \quad (4)$$

Here, the prime (as in g') denotes a derivative with respect to ρ . This result can be regarded as applying a ‘‘torque’’ to the step to produce a rotation $\theta = \tan^{-1} m$ from the minimum-energy, close-packed orientation.¹⁴

Taking the logarithm of Eq. (3), we find the projected free energy per column $f(m)$ as a Legendre transform of the reduced Gibbs free energy per column $g(\rho_0)$:

$$\frac{f(m)}{k_B T} \approx \rho_0 m + \frac{g(\rho_0)}{k_B T}. \quad (5)$$

Note that this expression is valid only for $L \gg 1$; for finite-sized systems, corrections are required. As standard for Legendre transforms,¹⁷ we have

$$\frac{\ddot{f}(m)}{k_B T} = -\frac{k_B T}{g''(\rho_0)}, \quad (6)$$

where $\ddot{f} \equiv \partial^2 f / \partial m^2$. Using $\beta(\theta)a = f(m) \cos \theta$ and $m = \tan \theta$, with a the lattice constant of the square (i.e., the column spacing, which is $1/\sqrt{2}$ the conventional fcc lattice constant), we can rewrite the stiffness as

$$\tilde{\beta}(\theta)a = \ddot{f}(m)/\cos^3 \theta, \quad (7)$$

or, similar to results by Bartelt *et al.*,⁸

$$\frac{k_B T}{\tilde{\beta}(\theta)a} = -\frac{g''(\rho_0)}{k_B T} \cos^3 \theta. \quad (8)$$

Thus, we only need $g''(\rho)$ to find the stiffness as a function of m or θ .

Of course, ρ_0 in g'' must be eliminated in favor of m via Eq. (4). The details for the general case are somewhat involved. Here, we simplify to the physically relevant case of $U = D$ and, defining $S \equiv H + U + D = H + 2D$, just quote the results:

$$\frac{g''(\rho_0)}{k_B T} = -m \left[\frac{2 \sinh \rho_0}{C(S, \rho_0)} + \coth \rho_0 \right] + m^2, \quad (9)$$

where $C(S, \rho_0) \equiv \cosh S - \cosh \rho_0$ and $\rho_0(m)$ is found by inverting

$$m = \frac{\sinh \rho_0 \sinh S}{C(S, \rho_0) [\sinh S - C(S, \rho_0)(1 - e^{-2D})]}. \quad (10)$$

Some details can be found in the Appendix. Since Eq. (10) is a quartic equation for $\cosh \rho_0$ or e^{ρ_0} , the explicit expression for $\rho_0(m)$ is rather opaque. However, at low-temperatures, a simpler formula emerges, as shown in the next section.

III. LOW-T SOLUTION: SIMPLE EXPRESSION

At low temperatures, we find that the appropriate root for ρ_0 diverges. Then we can write $\cosh \rho_0 \approx \sinh \rho_0 \approx e^{\rho_0}/2$. Of course, $H \propto 1/T$ so that $\cosh S \approx e^S/2$. With these approximations, Eq. (10) becomes quadratic in e^{ρ_0} :

$$m = \frac{e^{\rho_0+S}}{(e^S - e^{\rho_0})[e^S - (e^S - e^{\rho_0})(1 - e^{-2D})]}. \quad (11)$$

Likewise, the expression for $g''(\rho_0)$, Eq. (9), becomes

$$\frac{g''(\rho_0)}{k_B T} = -m \left[\frac{2e^{\rho_0}}{(e^S - e^{\rho_0})} + 1 \right] + m^2. \quad (12)$$

Solving for e^{ρ_0} in Eq. (11) and inserting the solution into Eq. (12) gives

$$\frac{g''(\rho_0)}{k_B T} = -m \sqrt{(1-m)^2 + 4me^{-2D}}. \quad (13)$$

so that, from Eq. (8), and recalling $D = -\epsilon_2/2k_B T$, we arrive at our *main result*, a simple, algebraic expression for $\tilde{\beta}$ as a function of m :

$$\frac{k_B T}{\tilde{\beta} a} = \frac{m \sqrt{(1-m)^2 + 4me^{\epsilon_2/k_B T}}}{(1+m^2)^{3/2}}. \quad (14)$$

We examine Eq. (14) in several different limiting cases. When $\epsilon_2=0$, this reduces to

$$\frac{k_B T}{\tilde{\beta} a} = \frac{m + m^2}{(1+m^2)^{3/2}}, \quad (15)$$

as found in a previous study involving only NN interactions.⁶ Interestingly, at $\theta=45^\circ$, Eq. (14) shows a simple dependence on ϵ_2 , namely,

$$\frac{k_B T}{\tilde{\beta} a} = \frac{e^{\epsilon_2/2k_B T}}{\sqrt{2}}. \quad (16)$$

Of course, this reduces to the venerable Ising result of $1/\sqrt{2}$ in the absence of NNN interactions ($\epsilon_2=0$).^{3,18,19}

By considering just the lowest and second lowest energy configurations,^{9,10} Zandvliet *et al.* obtained the result¹⁰ (expressed with our sign convention for ϵ_2) for the maximally misoriented case $m=1$,

$$\frac{k_B T}{\tilde{\beta} a} = \frac{\sqrt{2}}{1 + e^{-\epsilon_2/2k_B T}}, \quad (17)$$

which has, for the attractive ϵ_2 of primary concern here, some qualitative similarities to Eq. (16) (including the value $1/\sqrt{2}$ for $\epsilon_2=0$) but is too small by a factor of 2 for $\epsilon_2/2k_B T \ll 0$; even the coefficient of the first-order term in an expansion in $\epsilon_2/2k_B T$ is half the correct value. For the opposite limit of repulsive ϵ_2 , Eq. (17) levels off (at $\sqrt{2}$), in qualitative disagreement with the actual exponential increase seen in Eq. (16).

Figure 2 compares Eq. (14) to corresponding exact solutions [found by numerically solving Eqs. (8)–(10)] at several temperatures when $\epsilon_2 = \epsilon_1/10$. We see that Eq. (14) overlaps the exact solution at temperatures as high as $T_c/6$. As the temperature increases, the stiffness becomes more isotropic, and Eq. (14) begins to overestimate the stiffness near $\theta=0^\circ$. Of course, Eqs. (8)–(10) can be used to find the exact SOS stiffness at $T=0$. In agreement with previous calculations,^{7,13} we find

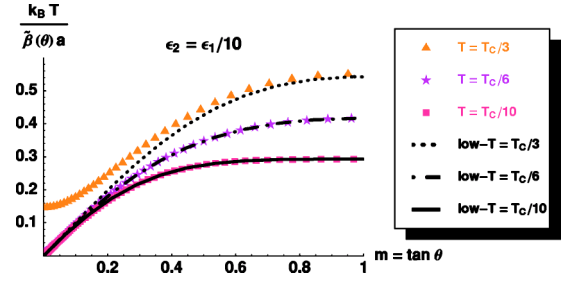


FIG. 2. The range of validity of Eq. (14) is examined by comparing it to exact numerical solutions of the SOS model at several temperatures. In the legend T_c refers to the NN lattice-gas (Ising) model; for $|\epsilon_1|=256$ meV, $T_c=1685$ K.

$$\frac{k_B T}{\tilde{\beta}(0)a} = \frac{\sinh S}{C(S,0)[\sinh S - C(S,0)(1 - e^{-2D})]}.$$

Finally, in Fig. 3 (using the experimental value²⁰ $\epsilon_k = 128$ meV $\Rightarrow \epsilon_1 = -256$ meV), we compare Eq. (14) to the NN Ising model at $T=320$ K, as well as to the experimental results of Ref. 6. For strongly attractive (negative) ϵ_2 , $k_B T/\tilde{\beta} a$ decreases significantly. In fact, when ϵ_2/ϵ_1 is $1/6$, so that $-\epsilon_2/2k_B T = (\epsilon_2/\epsilon_1)(\epsilon_k/k_B T) \approx (1/6)4.64$, the model-predicted value of $k_B T/\tilde{\beta} a$ has decreased to less than half its $\epsilon_2=0$ value [viz., by a factor of 0.46, versus 0.63 if Eq. (17) is used], so about $3/2$ the experimental ratio. If ϵ_2/ϵ_1 increases even further, $k_B T/\tilde{\beta} a$ further decreases and develops positive curvature, causing an end-point local minimum to appear at $\theta=45^\circ$. We can determine when this occurs by expanding Eq. (14) about $m=1$:

$$\frac{k_B T}{\tilde{\beta} a} = \frac{e^{-D}}{\sqrt{2}} + \left(\frac{e^D}{8\sqrt{2}} - \frac{3e^{-D}}{4\sqrt{2}} \right) (m-1)^2 + \dots \quad (18)$$

Setting the coefficient of $(m-1)^2$ to zero gives $-2D = \epsilon_2/k_B T = -\ln(6) \approx -1.8$, which corresponds to a value of

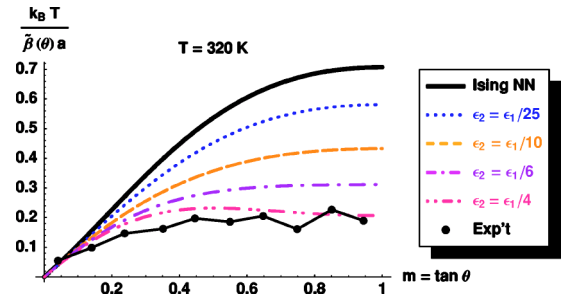


FIG. 3. Equation (14) is plotted for a variety of different values of $D = -\epsilon_2/2k_B T$, where ϵ_1 and ϵ_2 are NN- and NNN-interaction energies, respectively, in a lattice-gas picture. The solid curve denoted “Ising NN” corresponds to $\epsilon_2=0$. The dots labeled “Exp’t” are taken from Fig. 2 of Ref. 6 and were derived from the equilibrium shape of islands on Cu(001) at 302 K, with the line segments serving as guides for the eye. To minimize clutter, we omit similar data derived from correlation functions of vicinal surfaces at various temperatures. Note that for $\epsilon_2 = \epsilon_1/4$ a maximum has developed near $\tan \theta = 1/2$ that is not evident in the experimental data.

$k_B T / \tilde{\beta} a = \sqrt{3}/6 \approx 0.29$, about 2/5 the value at $\epsilon_2=0$. For $T=320$ K and $\epsilon_k=128$ meV, this corresponds to $\epsilon_2/\epsilon_1 \approx 0.2$. However, for the NNN interaction alone to account for the factor-of-4 discrepancy between model/theory and experiment reported by Dieluweit *et al.*,⁶ Fig. 3 shows that $\epsilon_2/\epsilon_1 \approx 0.3$ would be required.

IV. EFFECT OF TRIO INTERACTIONS

In addition to the NNN interaction, trio (three-atom, non-pairwise) interactions may well influence the stiffness. The strongest such interaction is most likely that associated with three atoms forming a right isosceles triangle, whose sides are at NN distance and hypotenuse at NNN separation. In a lattice-gas model, there is a new term with ϵ_{RT} times the occupation numbers of the three sites.¹² Note that this trio interaction energy ϵ_{RT} is in addition to the contribution $2\epsilon_1 + \epsilon_2$ of the constituent pair interactions. If we count broken trios and weight each by R , we find an additional contribution to Eq. (1) of R times,

$$4|\Delta_i| + 2\delta_{\Delta_i,0} + 2 = 2|\Delta_i| + |\Delta_i + 1| + |\Delta_i - 1| + 2, \quad (19)$$

where we have converted the Kronecker delta at $i=0$ to make better contact with Eq. (1). Thus, without further calculation we can include the effect of this trio by replacing H by $H + 2R$, U by $U + R$, D by $D + R$, and (trivially) V by $V + 2R$.

By arguments used at the end of Sec. II A, we recognize $R = -\frac{1}{2}\epsilon_{RT}$. Consequently, the effective NN lattice-gas energy is $\epsilon_1 + 2\epsilon_{RT}$ and, more significantly the effective NNN interaction energy is $\epsilon_2 + \epsilon_{RT}$. Thus, ϵ_{RT} must be attractive (negative) if it is to help account for the discrepancy in Fig. 2 of Ref. 6 between model and experiment. Furthermore, by revisiting the configurations discussed in the penultimate paragraph of the Introduction, we find that the kink energy ϵ_k becomes $-\frac{1}{2}\epsilon_1 - \epsilon_{RT}$. Thus, for a repulsive ϵ_{RT} , $|\epsilon_1|$ will be larger than predicted by an analysis of, e.g., step-edge diffusivity that neglects ϵ_{RT} . Lastly, the close-packed edge energy, i.e. the $T=0$ line tension $\beta(0) = -\frac{1}{2}\epsilon_1 - \epsilon_2$, becomes $-\frac{1}{2}\epsilon_1 - \epsilon_2 - 2\epsilon_{RT}$.

V. DISCUSSION AND CONCLUSIONS

We now turn to experimental information about the interactions, followed by comments on the limited available calculations of them, often recapitulating the discussion in Ref. 9. All the experiments are predicated on the belief that at 320 K there is sufficient mobility to allow equilibrium to be achieved. If the NNN interactions are to explain at least partially the high stiffness of experiment compared to Ising theory, the NNN interaction must be attractive and a substantial fraction of ϵ_1 . Since compact islands do form on the Cu(001) surface, it is obvious that ϵ_1 is attractive. If ϵ_2 is also attractive, as required for reduction of the overestimate of $k_B T / \tilde{\beta}$, then the low-temperature equilibrium shape has clipped corners (octagonal-like, with sides of alternating lengths), as noted in Ref. 9; no evidence of such behavior has been seen. The lack of evidence of a decreasing stiffness near $\theta \approx 45^\circ$ suggests that ϵ_2/ϵ_1 is at most 1/5.

There is implicit experimental information for ϵ_2 : from island shapes¹⁸ and fluctuations²¹ $\beta(0) = 220 \pm 11$ meV. Since related measurements showed $\frac{1}{2}\epsilon_1 = -128$ meV, we deduce $\epsilon_2 = -92$ meV if ϵ_{RT} is insignificant. These values imply that ϵ_2/ϵ_1 is somewhat larger than 1/3, which seems unlikely in light of the unobserved predictions about the shape of islands in that case (cf. the end of Sec. III).

To corroborate this picture, one should estimate the values of ϵ_1 and ϵ_2 , as well as ϵ_{RT} , from first-principles total-energy calculations. In contrast to Cu(111),^{22,23} however, no such information even for ϵ_1 has been published for Cu(001); there are, however, several semiempirical calculations which found $\epsilon_k \approx 0.14$ eV.²⁴ In such calculations based on the embedded atom method (EAM), which work best for late transition and noble fcc metals, the indirect ("through-substrate") interactions are expected to be strong only when the adatoms share common substrate nearest neighbors; then the interaction should be repulsive and proportional to the number of shared substrate atoms.²⁵ (Longer range pair interactions and multisite nonpairwise interactions are generally very-to-negligibly small in such calculations; they probably underestimate the actual values of these interactions since there is no Fermi surface in this picture, and it is the Fermi wavevector that dominates long-range interactions.) If the NN and NNN interactions on Cu(001) were purely indirect, we would then predict $\epsilon_2 = \frac{1}{2}\epsilon_1 > 0$. However, whenever direct interactions (due to covalent effects between the nearby adatoms) are important, they overwhelm the indirect interaction. At NN separation, which is the bulk NN spacing, direct interactions must be significant, explaining why ϵ_1 can be attractive. It is not obvious from such general arguments whether there are significant direct interactions between Cu adatoms at NNN separations. [For Pt atoms on Pt(100), the only homoepitaxial case in which ϵ_2 was computed semiempirically, EAM calculations²⁶ gave $\epsilon_2/|\epsilon_1| = 0.2$, less than half the ratio predicted by counting substrate neighbors, but with the predicted repulsive ϵ_2 .] It is also not obvious *a priori* whether multi-atom interactions also contribute significantly. [For homoepitaxy, the only semiempirical result is that they are insignificant for Ag on Ag(001);²⁷ however, it is likely that semiempirical calculations will underestimate multiatom interactions.]

To address these questions, we are currently carrying out calculations²⁸ using the VASP package.²⁹ Preliminary results for Cu(001) suggest that ϵ_2 is indeed attractive, and that ϵ_2/ϵ_1 is about 1/8; there are also indications of an attractive right-triangle trio interaction ϵ_{RT} with sizable magnitude (perhaps comparable to $|\epsilon_2|$, consistent with *a priori* expectations^{25,30}), but there is also a sizeable colinear trio interaction which is repulsive.

In summary, NNN interactions may well account for a significant fraction, perhaps even a majority, of the discrepancy between NN Ising model calculations and experimental measurements of the orientation dependence of the reduced stiffness;⁶ the effect is even somewhat greater than estimated by the Twente group.^{9,10} However, inclusion of ϵ_2 is not the whole answer, nor, seemingly, is consideration of ϵ_{RT} . One possible missing ingredient is other multisite interactions, most notably the linear trio ϵ_{LT} consisting of three colinear atoms (a pair of NN legs and an apex angle of 180°). In a

model calculation their energy was comparable to ϵ_{RT} ,^{25,30} albeit with half as many occurrences per atom in the monolayer phase. The corrections due to ϵ_{LT} would be more complicated than simple shifts in the effective values of ϵ_1 and ϵ_2 . Since direct interactions are probably important, there is no way to escape doing a first-principles computation; we continue to use the VASP package to extend our preliminary calculations.²⁸ A more daunting (at least for lattice-gas aficionados) possibility is that long-range intrastep elastic effects may be important. Shenoy and Ciobanu have made noteworthy progress in understanding how this interaction contributes to the orientation dependence of noble-metal steps.³¹

ACKNOWLEDGMENTS

Work at the University of Maryland was supported by the NSF-MRSEC, Grant No. DMR 00-80008. One of us (R.K.P.Z.) acknowledges support by NSF Grants No. DMR 00-88451 and 04-14122. T.L.E. acknowledges partial support of collaboration with ISG at FZ-Jülich via the Humboldt Foundation. We have benefited from ongoing interactions with E. D. Williams and her group.

APPENDIX: CALCULATIONAL DETAILS

1. Partition function

To carry out the sum in Eq. (2), we consider the Fourier transform of $Z(Y)$:

$$\begin{aligned} W(\mu) &\equiv \int_{-\infty}^{\infty} dY e^{i\mu Y} Z(Y) = \sum_{\{\Delta\}} \exp \sum_{j=1}^L [i\mu\Delta_j - K(\Delta_j)] \\ &= \left[\sum_{\Delta=-\infty}^{\infty} \exp[i\mu\Delta - K(\Delta)] \right]^L, \end{aligned} \quad (\text{A1})$$

where $K(\Delta) \equiv (V+H|\Delta|+U|\Delta-1|+D|\Delta+1|)$ is the energy in Eq. (1), associated with adjacent columns with height difference Δ . Carrying out the summation in Eq. (A1) gives

$$\frac{g(i\mu)}{k_B T} \equiv -\frac{1}{L} \ln W(i\mu) = V + U + D - \ln B(i\mu), \quad (\text{A2})$$

where

$$B(i\mu) \equiv 1 + \frac{e^{2D}}{e^{H+U+D+i\mu} - 1} + \frac{e^{2U}}{e^{H+U+D-i\mu} - 1}. \quad (\text{A3})$$

Thus, the original partition function $Z(Y)$ is

$$\begin{aligned} Z(Y) &= \frac{1}{2\pi} \int_{-\infty}^{\infty} d\mu e^{-i\mu Y} W(\mu) \\ &= \frac{1}{2\pi} \int_{-\infty}^{\infty} d\mu \exp \left[L \left(-i\mu \tan \theta - \frac{g(i\mu)}{k_B T} \right) \right] \end{aligned} \quad (\text{A4})$$

For $L \gg 1$, we can evaluate this inverse transform by steepest decent approximation. The saddle point occurs on the imagi-

nary axis ($\mu = -i\rho$), at the value ρ_0 given by the stationary-phase condition:

$$-\frac{g'(\rho_0)}{k_B T} = m \equiv \tan \theta. \quad (\text{A5})$$

Calculating the derivative from Eqs. (A2) and (A3), we find

$$m = B'(\rho_0)/B(\rho_0), \quad (\text{A6})$$

where prime stands for ∂_ρ . The leading contribution to this integral (A4) is just the integrand evaluated at this point:

$$Z(Y) \approx \exp \left[-L \left(m\rho_0 + \frac{g(\rho_0)}{k_B T} \right) \right]. \quad (\text{A7})$$

2. Analysis of $g''(\rho)$ and specialization to $U=D$

From Eqs. (A2), we find

$$\frac{g'(\rho)}{k_B T} = -B'(\rho)/B(\rho) \quad (\text{A8})$$

and

$$\frac{g''(\rho)}{k_B T} = -B''(\rho)/B(\rho) + [B'(\rho)/B(\rho)]^2. \quad (\text{A9})$$

This can be simplified, by Eq. (A6), to

$$\frac{g''(\rho_0)}{k_B T} = -mB''(\rho_0)/B'(\rho_0) + m^2, \quad (\text{A10})$$

the quantity needed for computing the stiffness as a function of m . While straightforward, computing the derivatives with the general form for B [Eq. (A3) with $\rho = i\mu$] is quite tedious. A slight simplification emerges if we specialize to the physically relevant case $U=D$. Then, with $S \equiv H+2D$, we have

$$\begin{aligned} B(\rho) &= 1 + \frac{e^{2D}}{e^{S+\rho} - 1} + \frac{e^{2D}}{e^{S-\rho} - 1} = 1 - e^{2D} + \frac{e^{2D} \sinh S}{\cosh S - \cosh \rho} \\ &\equiv 1 - e^{2D} + \frac{e^{2D} \sinh S}{C(S, \rho)}, \end{aligned} \quad (\text{A11})$$

so that

$$B'(\rho) = e^{2D} \sinh S \frac{\sinh \rho}{C^2(S, \rho)}, \quad (\text{A12})$$

and

$$B''(\rho) = e^{2D} \sinh S \left[\frac{\cosh \rho}{C^2(S, \rho)} + \frac{2 \sinh^2 \rho}{C^3(S, \rho)} \right]. \quad (\text{A13})$$

Inserting these expressions into Eq. (A6), we have

$$m = \frac{\sinh \rho_0 \sinh S}{C(S, \rho_0) [\sinh S - C(S, \rho_0)(1 - e^{-2D})]}. \quad (\text{A14})$$

Similarly, with Eq. (A10), we find

$$\frac{g''(\rho_0)}{k_B T} = -m \left[\frac{2 \sinh \rho_0}{C(S, \rho_0)} + \coth \rho_0 \right] + m^2. \quad (\text{A15})$$

*Electronic address: tjs@glue.umd.edu

†Corresponding author. Electronic address: einstein@umd.edu

- ¹H.-C. Jeong and E. D. Williams, *Surf. Sci. Rep.* **34**, 171 (1999).
- ²This simple equivalency does not hold for stepped surfaces in an electrochemical system, where the electrode potential ϕ is fixed rather than the surface charge density conjugate to ϕ . H. Ibach and W. Schmickler, *Phys. Rev. Lett.* **91**, 016106 (2003).
- ³C. Rottman and M. Wortis, *Phys. Rev. B* **24**, 6274 (1981).
- ⁴J.E. Avron, H. van Beijeren, L. S. Schulman, and R. K. P. Zia, *J. Phys. A* **15**, L81 (1982); R.K.P. Zia and J.E. Avron, *Phys. Rev. B* **25**, 2042 (1982).
- ⁵J.W. Cahn and R. Kikuchi, *J. Phys. Chem. Solids* **20**, 94 (1961).
- ⁶S. Dieluweit, H. Ibach, M. Giesen, and T. L. Einstein, *Phys. Rev. B* **67**, 121410 (2003).
- ⁷N. Akutsu and Y. Akutsu, *Surf. Sci.* **376**, 92 (1997).
- ⁸N. C. Bartelt, T. L. Einstein, and E. D. Williams, *Surf. Sci.* **276**, 308 (1992).
- ⁹R. Van Moere, H. J. W. Zandvliet, and B. Poelsema, *Phys. Rev. B* **67**, 193407 (2003).
- ¹⁰H. J. W. Zandvliet, R. Van Moere, and B. Poelsema, *Phys. Rev. B* **68**, 073404 (2003).
- ¹¹R. C. Nelson, T. L. Einstein, S. V. Khare, and P. J. Rous, *Surf. Sci.* **295**, 462 (1993).
- ¹²Explicitly, the contribution to the lattice-gas Hamiltonian of all NN bonds is $\epsilon_1 \sum_{\langle i,j \rangle} n_i n_j$, where the site-occupation variable $n_i = 0, 1$, and the summation is over all NN pairs of sites. It is well known that $\epsilon_1 \rightarrow -4J_1$ in the corresponding Ising model, so that T_c is determined by $\sinh(|\epsilon_1|/2k_B T) = 1$. Unfortunately, the variety of notations in papers on this subject can lead to confusion. In Refs. 9 and 10, $\epsilon_{1,2}$ have the opposite sign of our $\epsilon_{1,2}$. In Ref. 17 and somewhat implicitly in Ref. 6, the so-called the Ising parameter, ϵ , is $\epsilon_k = 2J = -\frac{1}{2}\epsilon_1$.
- ¹³W. K. Burton, N. Cabrera, and F. C. Frank, *Philos. Trans. R. Soc. London, Ser. A* **243**, 299 (1951).
- ¹⁴H. J. Leamy, G. H. Gilmer, and K. A. Jackson, in *Surface Physics of Materials*, edited by J. M. Blakely (Academic, New York, 1975), Vol. 1, p. 121.
- ¹⁵T. W. Burkhardt, *Z. Phys. B* **29**, 129 (1978).
- ¹⁶H. J. W. Zandvliet, H. B. Elswijk, E. J. van Loenen, and D. Dijkkamp, *Phys. Rev. B* **45**, 5965 (1992).
- ¹⁷While this issue is treated in textbooks, a more readily accessible exposition of the negative reciprocal relationship between the field and conjugate density susceptibilities is given (in an introductory review couched in magnetic language) by M. Kollar, I. Spremo, and P. Kopietz, *Phys. Rev. B* **67**, 104427 (2003).
- ¹⁸M. Giesen, C. Steimer, and H. Ibach, *Surf. Sci.* **471**, 80 (2001).
- ¹⁹H. J. W. Zandvliet, *Phys. Rev. B* **61**, 9972 (2000).
- ²⁰M. Giesen-Seibert and H. Ibach, *Surf. Sci.* **316**, 205 (1994); M. Giesen-Seibert, F. Schmitz, R. Jentjens, and H. Ibach, *ibid.* **329**, 47 (1995).
- ²¹C. Steimer, M. Giesen, L. Verheij, and H. Ibach, *Phys. Rev. B* **64**, 085416 (2001).
- ²²A. Bogicevic, S. Ovesson, P. Hyldgaard, B. I. Lundqvist, H. Brune, and D. R. Jennison, *Phys. Rev. Lett.* **85**, 1910 (2000).
- ²³P. J. Feibelman, *Phys. Rev. B* **60**, 11118 (1999).
- ²⁴Using EAM, C. S. Liu and J. B. Adams, *Surf. Sci.* **294**, 211 (1993) found $\epsilon_k = 139$ meV. Using a pair-potential expansion from a first-principles database of surface energies, L. Vitos, H. L. Skriver, and J. Kollár, *ibid.* **425**, 212 (1999) obtained $\epsilon_k = 163$ meV. With an *spd* tight-binding model, F. Raouafi, C. Barreteau, M. C. Desjonquères, and D. Spanjaard, *ibid.* **505**, 183 (2002) calculated $\epsilon_k = 146$ meV.
- ²⁵T. L. Einstein, in *Handbook of Surface Science*, edited by W. N. Unertl (Elsevier Science, Amsterdam, 1996), Vol. 1, Chap. 11.
- ²⁶A. F. Wright, M. S. Daw, and C. Y. Fong, *Phys. Rev. B* **42**, 9409 (1990).
- ²⁷I. Vattulainen (unpublished); in conjunction with J. Merikoski, I. Vattulainen, J. Heinonen, and T. Ala-Nissila, *Surf. Sci.* **387**, 167 (1997).
- ²⁸T. J. Stasevich, T. L. Einstein, and S. Stolbov (unpublished).
- ²⁹G. Kresse and J. Hafner, *Phys. Rev. B* **47**, 558 (1993); **49**, 14 251 (1994); G. Kresse and J. Furthmüller, *Comput. Mater. Sci.* **6**, 15 (1996); *Phys. Rev. B* **54**, 11169 (1996).
- ³⁰T. L. Einstein, *Langmuir* **7**, 2520 (1991); *Surf. Sci.* **84**, 497 (1979).
- ³¹V.B. Shenoy and C.V. Ciobanu, *Surf. Sci.* **554**, 222 (2004).